arXiv:1209.4702v1 [astro-ph.CO] 21 Sep 2012

revised submitted to ApJ, on September 24, 2012

What governs the bulk velocity of the jet components in active galactic nuclei?

Bo Chai, Xinwu Cao and Minfeng Gu

Key Laboratory for Research in Galaxies and Cosmology, Shanghai Astronomical Observatory, Chinese Academy of Sciences, 80 Nandan Road, Shanghai, 200030, China; chaibo@shao.ac.cn;cxw@shao.ac.cn;gumf@shao.ac.cn

ABSTRACT

We use a sample of radio-loud active galactic nuclei (AGNs) with measured black hole masses to explore the jet formation mechanisms in these sources. Based on the Königl's inhomogeneous jet model, the jet parameters, such as the bulk motion Lorentz factor, magnetic field strength, and electron density in the jet, can be estimated with the very long-baseline interferometry and X-ray data. We find a significant correlation between black hole mass and the bulk Lorentz factor of the jet components for this sample, while no significant correlation is present between the bulk Lorentz factor and the Eddington ratio. The massive black holes will be spun up through accretion, as the black holes acquire mass and angular momentum simultaneously through accretion. Recent investigation indeed suggested that most supermassive black holes in elliptical galaxies have on average higher spins than the black holes in spiral galaxies, where random, small accretion episodes (e.g., tidally disrupted stars, accretion of molecular clouds) might have played a more important role. If this is true, the correlation between black hole mass and the bulk Lorentz factor of the jet components found in this work implies that the motion velocity of the jet components is probably governed by the black hole spin. No correlation is found between the magnetic field strength at $10R_{\rm S}$ ($R_{\rm S}=2GM/c^2$ is the Schwarzschild radius) in the jets and the bulk Lorentz factor of the jet components for this sample. This is consistent with the black hole spin scenario, i.e., the faster moving jets are magnetically accelerated by the magnetic fields threading the horizon of more rapidly rotating black holes. The results imply that the Blandford-Znajek (BZ) mechanism may dominate over the Blandford-Payne (BP) mechanism for the jet acceleration at least in these radio-loud AGNs.

Subject headings: galaxies:active– galaxies:jets–galaxies: magnetic fields

1. Introduction

Only a small fraction of active galactic nuclei (AGNs) are radio-loud (e.g., Kellermann et al. 1989). Relativistic jets have been observed in many radio-loud AGNs, which are believed to be formed very close to black holes. The power of jets is supposed to be extracted from the accretion disk or the rotating black hole. The currently most favored models of jet formation are Blandford-Znajek (BZ) and Blandford-Payne (BP) mechanisms (Blandford & Znajek 1977; Blandford & Payne 1982). In the BZ process, energy and angular momentum are extracted from a rotating black hole and transferred to a remote astrophysical load by open magnetic field lines. In the BP process, the magnetic field threading the disk extracts energy from the rotating gas in the accretion disk to power the jet/outflow. The relative importance of these two mechanisms has been extensively explored by many different authors, which is still debating (e.g., Moderski & Sikora 1996; Livio et al. 1999; Cao 2011).

The apparent motions of the jet components in AGNs were detected by multi-epoch very long-based interferometry (VLBI) observations (e.g., Kellermann et al. 2004; Lister & Homan 2005). The Lorentz factor and the viewing angle of the jet component can be derived with the measured proper motion of the jet component if the Doppler factor is estimated. There are several different approaches applied to estimate the Doppler factor of the jets. Readhead (1994) estimated the equipartition Doppler boosting factor assuming that the sources are in equipartition between the energy of radiating particles and the magnetic field in the jets (also see Guijosa & Daly 1996). The variability Doppler factor is derived on the assumption that the associated variability brightness temperature of total radio flux density flares are caused by the relativistic jets (Lähteenmäki & Valtaoja 1999). Based on the synchrotron self-Compton (SSC) model, the physical quantities in the jets can be estimated by using the VLBI observations and the X-ray flux density on the assumption of homogeneous spherical emission plasma (Marscher 1987; Ghisellini et al. 1993). The inhomogeneous relativistic jet model can reproduce both the flat spectrum characteristics of some AGNs and the dependence of the core size on the observing frequency (Blandford & Königl 1979; Königl 1981). Based on this inhomogeneous jet model, an approach was suggested by Jiang et al. (1998) to estimate the jet parameters including bulk Lorentz factor Γ, viewing angle θ, and electron number density $n_{\rm e}$ in the jets of AGNs.

The relation between the jets and the accretion disks were extensively explored in many previous works (e.g., Rawlings et al. 1989; Celotti et al. 1997; Cao & Jiang 1999, 2001; Gu et al. 2009), which indicate the jets are indeed closely linked to the accretion disks, though the different jet formation mechanisms are still indistinguishable. The relationship between black hole mass and the motion of the jet components for a sample of blazars with measured proper motion of jet components by multi-epoch VLBI observations was investigated by Zhou & Cao (2009). They found a significant intrinsic correlation between black hole masses and the minimal Lorentz factors of the jet components, while the Eddington ratio is only weakly correlated with the minimal Lorentz factor. They suggested that the BZ mechanism may dominate over the BP mechanism for the jet acceleration at least in these blazars, if massive black holes are spinning more rapidly than their less massive counterparts.

In this work, we use a sample of radio-loud AGNs with jet parameters estimated with the inhomogeneous jet model to re-investigate the relationship of the Lorentz factor of jets with black hole mass, the Eddington ratio, or the strength of the magnetic field in the jets. The sample and the physical parameters used in this paper are described in Section 2. Section 3 contains the results. The last section includes the discussion. The cosmology with $H_0 = 70$ km s^{-1} Mpc^{-1}, $\Omega_{\rm M} = 0.3$, and $\Omega_\Lambda = 0.7$ have been adopted throughout this work.

2. Estimate of the jet parameters

Based on the Königl's inhomogeneous jet model, the jet parameters including the bulk Lorentz factor Γ, viewing angle θ, and electron number density $n_{\rm e}$ in the jets can be estimated with the data of VLBI and X-ray observations. We summarize the inhomogeneous jet model and the approach used to estimate the jet parameters in this section (see Jiang et al. 1998; Gu et al. 2009, for the details).

Königl (1981) constructed an inhomogeneous jet model, in which the magnetic field strength and number density of the relativistic electrons are assumed to vary with the distance from the apex of the jet r as $B(r) = B_1(r/r_1)^{-m}$ and $n_{\rm e}(r, \gamma_{\rm e}) = n_1(r/r_1)^{-n}{\gamma_{\rm e}}^{-(2\alpha+1)}$ in the jet, respectively, where $r_1 = 1$ pc and $\gamma_{\rm e}$ is the Lorentz factor of the electron in the jet. In this jet model, the conical jet with a half opening angle ϕ is moving in the direction at a viewing angle of θ with respect to line of sight. The distance $r(\tau_{\nu_{\rm s}} = 1)$, at which the optical depth to the synchrotron self-absorption at the observing frequency $\nu_{\rm s}$ equals unity, is given by

$$\frac{r(\tau_{\nu_{\rm s}} = 1)}{r_1} = (2c_2(\alpha)r_1 n_1 \phi \csc\theta)^{2/(2\alpha+5)k_{\rm m}} (B_1\delta)^{(2\alpha+3)/(2\alpha+5)k_{\rm m}} (\nu_{\rm s}(1+z))^{-1/k_{\rm m}}, \tag{1}$$

where $c_2(\alpha)$ is the constant in the synchrotron absorption coefficient, δ is the Doppler factor, and $k_{\rm m} = [2n + m(2\alpha+3) - 2]/(2\alpha+5)$.

The optically thick VLBI core size corresponds to the projection of the distance $r(\tau_{\nu_{\rm s}} = 1)$, and therefore the VLBI core angular size $\theta_{\rm d}$ is

$$\theta_{\rm d} = \frac{r(\tau_{\nu_{\rm s}} = 1)\sin\theta}{D_{\rm a}}, \tag{2}$$

where $D_{\rm a}$ is the angular diameter distance of the source.

By integrating the observed intensity over the projected area of the jet, the total optically thick flux is

$$s(\nu_{\rm s}) = \frac{r_1^2\phi\sin\theta}{(4+m)\pi D_{\rm a}^2}\frac{c_1(\alpha)}{c_2(\alpha)}B_1^{-1/2}\nu_{\rm s}^{5/2}\left(\frac{\delta}{1+z}\right)^{1/2}\left(\frac{r(\tau_{\nu_{\rm s}}=1)}{r_1}\right)^{(4+m)/2}, \tag{3}$$

where $\nu_{\rm s}$ is the VLBI observing frequency, and $c_1(\alpha)$ and $c_2(\alpha)$ are the constants in the synchrotron emission and absorption coefficients, respectively. The relation between apparent transverse velocity $\beta_{\rm app}$ and the bulk velocity of the jet βc is

$$\beta_{\rm app} = \frac{\beta\sin\theta}{1-\beta\cos\theta}. \tag{4}$$

The X-ray flux density of the unresolved jet can be calculated with Equation (13) in Königl (1981)'s work. The frequency region $\nu_{\rm c} > \nu_{\rm cb}(r_{\rm M})$ was adopted, where $r_{\rm M}$ is the smallest radius from which optically thin synchrotron emission with spectral index α is observed (see Königl 1981, for the details).

Given the three parameters, α, m, and n, the four independent variables, n_1, B_1, β, and θ can be derived from Equations (2)-(4) together with Königl (1981)'s equation (13) by using the data of the VLBI and X-ray observations. The total electron number density $n_{\rm t}$ is given by

$$n_{\rm t} = \int\limits_{\gamma_{\rm min}}^{\gamma_{\rm max}} n_{\rm e}(r,\gamma_{\rm e})d\gamma_{\rm e}. \tag{5}$$

The model parameters, $\alpha = 0.75$, $m = 1$ and $n = 2$ are adopted in Gu et al. (2009) for a jet with mass conserved along r. The kinetic power of jet can be calculated with

$$L_{\rm kin} = \frac{4}{3}\pi r_1^2 n_1\gamma_{\rm e,min}^{-\frac{3}{2}}[1-\cos(1/\Gamma)]m_{\rm e}\langle\gamma_{\rm e}\rangle\Gamma(\Gamma-1)\beta c^3, \tag{6}$$

for electron-positron jets, and

$$L_{\rm kin} = \frac{4}{3}\pi r_1^2 n_1\gamma_{\rm e,min}^{-\frac{3}{2}}[1-\cos(1/\Gamma)](m_{\rm e}\langle\gamma_{\rm e}\rangle + m_{\rm p}\langle\gamma_{\rm p}\rangle)\Gamma(\Gamma-1)\beta c^3, \tag{7}$$

for electron-proton jets, where Γ is the Lorentz factor of the jet, $1/\Gamma$ is the half opening angle of the conical jet, $m_{\rm e}$ is the electron rest mass, $m_{\rm p}$ is the rest mass of proton, $\langle\gamma_{\rm e}\rangle$ is the average Lorentz factor of electrons, and $\langle\gamma_{\rm p}\rangle$ is the average Lorentz factor of protons. We have assumed the positrons have the same energy distribution as the electrons in electron-positron jets, which contribute a half portion of the observed emission from the jets. This means that the density n_e derived from the observational data based on the inhomogeneous jet model is the total number density of the electrons and positrons in the jets.

The composition of the jet plasma is still an unresolved issue. The Reynolds et al. (1996) analyzed VLBI data of M87 and concluded that the core is probably dominated by electron-positron plasma. By detecting circular polarization, Wardle et al. (1998) suggested that extragalactic radio jets are composed mainly of electron-positron plasma with $\gamma_{\rm e,min} \lesssim 10$. Considering the dynamic and radiation properties, Kino & Takahara (2004) and Hirotani (2005) suggested that the sources they studied are composed of electron-positron plasma. The presence of protons and the minimal energy of electrons in the hot spots of the radio lobes are constrained by multi-waveband observations (Blundell et al. 2006; Stawarz et al. 2007; Godfrey et al. 2009). Sikora & Madejski (2000) suggested that the X-ray spectral observations in OVV quasars require the composition of the jets to be a mixture of electrons-positrons and protons. The detailed calculations of the pressure of the cocoon in Cygnus A did not give a tight constraint on the jet composition, i.e., either electron-positron or electron-proton plasma is possible in the jets of this source (Kino et al. 2012). Faraday rotation is sensitive to the plasma composition, which can also be used to constrain the composition of jets (e.g., Park & Blackman 2010). It was found that the presence of protons is required to explain the observed circular polarization and Faraday rotation in radio cores of blazars (e.g., Vitrishchak et al. 2008; Park & Blackman 2010). For electron-proton jets, $\gamma_{\rm e,min} \sim 100$ is suggested, and the low cut-off energy of jet can be as low as unity for electron-positron jets (Celotti & Fabian 1993), while Wardle et al. (1998) suggested that the jets are electron-positron plasmas with $\gamma_{\rm e,min} \lesssim 10$ at least in some sources. For electron-proton jets, assuming the inverse Compton scattering origin of X-ray emission from PKS 0637−752, Tavecchio et al. (2000) find that, $\gamma_{\rm e,min} = 10$, if the seed photon come from radiation field external to the jets (e.g., the cosmic microwave background), or $\gamma_{\rm e,min} = 2 \times 10^3$ for the sychrontron self-Compton case. We note that only the normalization is changed if the different plasma composition is considered, which means that most of the statistic results derived in this work is independent of the jet composition. The kinetic power derived for electron-positron pair plasma is roughly consistent with that derived for electron-proton plasma with conventionally used minimal values of electron energy. The bulk kinetic power $L_{\rm kin}$ for an electron-proton jet with $\gamma_{\rm e,min} = 100$ is in agreement with that of electron-positron jets with $\gamma_{\rm e,min} = 10$ within a factor of 3, as $m_{\rm p} = 1836 m_{\rm e}$ and $\langle \gamma_{\rm p} \rangle = 1$ for electron-proton jets (Gu et al. 2009). We find that the kinetic luminosity $L_{\rm kin}$ will be reduced by about a factor of 3 if $\gamma_{\rm e,min}$ is changed from 10 to 1. The choice of matter composition of jets does not change the bulk kinetic power of jet significantly, and most of the statistic analyses are not affected by the matter composition of jets. For simplicity, we therefore calculate the bulk kinetic power $L_{\rm kin}$ assuming electron-positron jets with $\gamma_{\rm e,min} = 10$ in this work.

3. The sample

Gu et al. (2009) constructed a sample of 128 sources, of which the jet parameters are derived from the VLBI and X-ray data with the Königl's inhomogeneous jet model. We search the literature for the black hole mass measurements, and finally obtain a sample of 101 sources with measured black hole masses, including 77 quasars, 20 BL Lac objects and 4 radio galaxies. The black hole masses for most sources in our sample are estimated by using an empirical relation between BLR size and ionizing luminosity together with measured broad-line widths assuming the BLR clouds being gravitationally bound by the central black hole (e.g., Shields et al. 2003; Liu et al. 2006; Shen et al. 2008; Wu 2009; Zhou & Cao 2009). For some sources, especially BL Lac objects or radio galaxies, the black hole masses can be estimated from the properties of their host galaxies with either $M_{\rm BH}$-σ or $M_{\rm BH}$-L relations, where σ and L are the stellar velocity dispersion and the bulge luminosity of the host galaxies (e.g., Woo et al. 2005; Cao 2003). The black hole masses can also be estimated with the γ-ray variability timescales for some γ-ray blazars (Liang & Liu 2003). For a few sources, the black hole masses are estimated from reverberation mapping (Peterson et al. 2004) and stellar kinetics (Panessa et al. 2006)(see Table 1). The bolometric luminosity $L_{\rm bol}$ is estimated from the total broad-line luminosity by assuming $L_{\rm bol} = 10L_{\rm BLR}$ (Netzer 1990). All the data for the sample are summarized in Table 1, in which all the jet parameters are taken from Gu et al. (2009).

4. Results

We plot the relation between black hole mass and the bulk Lorentz factor of the jet components in Figure 1. A strong correlation is found between these two quantities with a Spearman rank correlation coefficient $r = 0.357$ at 99.98 percent confidence level. Using the linear regression analysis, the correlation can be expressed as

$$\log\Gamma = (0.20 \pm 0.06)\log M_{\rm BH} - (0.68 \pm 0.52), \tag{8}$$

and it becomes

$$\log\Gamma = (0.21 \pm 0.07)\log M_{\rm BH} - (0.70 \pm 0.61), \tag{9}$$

for the quasars in the sample with a correlation coefficient $r = 0.376$ at 99.92 percent confidence level.

In Figure 2, we plot the relation between black hole mass and redshift z, and the relation between the bulk Lorentz factor of the jet components and redshift z. It is found that both the black hole mass and the Lorentz factor are strongly correlated with redshift

z, which implies that the correlation between black hole mass and the bulk Lorentz factor of the jet components may be caused by the common dependence of redshift. We therefore choose a sub-sample of the sources in a restricted range of redshift $0.8 < z < 1.2$ (see the sources between two vertical dotted lines in Figure 2). No significant correlations are present between $M_{\rm BH}$ and z, or Γ and z, while a significant correlation between $M_{\rm BH}$ and Γ is still present for the sources in this sub-sample (see Figure 3 and Table 2). Therefore, we conclude that the significant correlation between black hole mass and the bulk Lorentz factor might be intrinsic, at least for our present sample, which is confirmed by the partial correlation analyses (see Table 2).

The relation between the Eddington ratio and the bulk Lorentz factor of the jet components is plotted in Figure 4. The correlation analysis shows that no significant correlation is found between $L_{\rm bol}/L_{\rm Edd}$ and Γ with a correlation coefficient $r = 0.099$ at 63.94 percent confidence level.

As the masses of the black holes in this sample are in the range of $\sim 10^7 - 10^{10} M_{\odot}$, we plot the relation of the bulk Lorentz factor of jet Γ with the magnetic field strength at $10R_{\rm S}$ in Figure 5. No correlation is found between these two quantities with a correlation coefficient $r = 0.01$ at 7.78 percent confidence level. We summarize the statistic results in Table 2.

We define jet efficiency $\eta_{\rm jet}$ as

$$L_{\rm kin} = \eta_{\rm jet} \dot{M}_{\rm acc} c^2, \tag{10}$$

where $\dot{M}_{\rm acc}$ is the mass accretion rate. The mass accretion rate can be estimated from the bolometric luminosity, i.e., $L_{\rm bol} = 0.1\dot{M}_{\rm acc}c^2$, and therefore,

$$\eta_{\rm jet} = \frac{0.1 L_{\rm kin}}{L_{\rm bol}}. \tag{11}$$

The distribution of the jet efficiency for our sample is given in Figure 6. It is found that the efficiencies of some sources are significantly greater than unity, which may be due to a fixed $\gamma_{\rm e,min}$ for all sources. The possibility of different values of $\gamma_{\rm e,min}$ in some individual sources cannot be ruled out (see the discussion in Section 2). The relation between the bolometric luminosity and the kinetic power of the jet is plotted in Figure 7. The magnetic energy density in the jets can be expressed as $U_{\rm B} = B^2/8\pi$, and the magnetic energy flux in the jets can be calculated with $B_1^2 r_1^2 c[1 - \cos(1/\Gamma)]\Gamma^2/4$. The ratio of the bulk kinetic power $L_{\rm kin}$ to the magnetic energy flux $L_{\rm B}$ in the jets is plotted in Figure 8.

5. Discussion

We find an intrinsic correlation between the black hole masses and the Lorentz factors of the jet components for a sample of radio-loud AGNs, while no significant correlation between the Eddington ratios and the Lorentz factors is present for the same sample. No correlation is found between the magnetic field strength at a given distance in units of Schwarzschild radius in the jet and the bulk Lorentz factor. These results provide useful clues on the mechanisms of jet formation and acceleration in radio-loud AGNs.

Mass accretion in the AGN phases plays a dominant role in the growth of massive black holes in the centers of galaxies (e.g., Soltan 1982; Tremaine et al. 2002). As massive black holes acquire mass and angular momentum simultaneously through accretion, the black holes will be spun up with mass growth. The mergers of black holes may also affect the spin evolution of massive black holes (Hughes & Blandford 2003). Volonteri et al. (2007) investigated how the accretion from a warped disc influences the evolution of black hole spins with the effects of accretion and merger being properly considered and concluded that within the cosmological framework, most supermassive black holes in elliptical galaxies have on average higher spins than black holes in spiral galaxies, where random, small accretion episodes (e.g., tidally disrupted stars, accretion of molecular clouds) might have played a more important role. Cao & Li (2008) calculated the black hole mass function of AGN relics with the observed Eddington ratio distribution of AGNs, and compared it with the measured mass function of the massive black holes in galaxies. They found that the radiative efficiencies of most massive accreting black holes are higher than those of less spinning black holes. If this is the case, the correlation between $M_{\rm BH}$ and Γ found in this work indicates that the bulk velocity of jets is mainly regulated by the black hole spin parameter a. The kinetic power of the jet is,

$$L_{\rm kin} = \Gamma \dot{M}_{\rm jet} c^2, \tag{12}$$

where $\dot{M}_{\rm jet}$ is the mass loss rate in the jet. If the jet is powered through the BZ process, we have

$$L_{\rm kin} \sim L_{\rm BZ} \propto M_{\rm BH} a^2, \tag{13}$$

for a radiation pressure dominated accretion disk surrounding a rotating black hole (Ghosh & Abramowicz 1997), where a is the black hole spin parameter. Combining Equations (11) and (12), we have

$$\Gamma \propto \left(\frac{\dot{M}_{\rm jet}}{M_{\rm BH}} \right)^{-1} a^2. \tag{14}$$

This indicates that the Lorentz factor of the jet Γ should be anti-correlated with $\dot{M}_{\rm acc}/M_{\rm BH}$ if $\dot{M}_{\rm jet} \propto \dot{M}_{\rm acc}$, which seems to be inconsistent with our statistic results. It implies that such a jet formation model for a radiation pressure dominated accretion disk may not be applicable for the blazars considered in this work. In fact, the structure of the radiation pressure dominated accretion disks should be altered significantly in the presence of strong magnetic fields (Li & Cao 2012), which was not considered in Ghosh & Abramowicz (1997).

Recent numerical simulations show that an accretion flow can evolve into a magnetically arrested flow, and at this state the outflow efficiency can be extremely high (as high as $\gtrsim$ 100%) (Tchekhovskoy et al. 2011; McKinney et al. 2012; Tchekhovskoy & McKinney 2012). The strength of the field in the magnetically arrested accretion flow can be estimated as (Tchekhovskoy et al. 2011; McKinney et al. 2012),

$$B^2 \propto \frac{\dot{M}_{\rm acc}}{M_{\rm BH}^2}. \tag{15}$$

If the jet is powered through the BZ process, we have

$$L_{\rm kin} \sim L_{\rm BZ} \propto M_{\rm BH}^2 B^2 a^2, \tag{16}$$

where a is the black hole spin parameter. Combining Equations (15) and (16), we obtain

$$L_{\rm kin} \propto \dot{M}_{\rm acc} a^2, \tag{17}$$

which implies

$$\eta_{\rm jet} \propto a^2. \tag{18}$$

Hence, the efficiency of the jet production does not depend on the accretion rate of the disk. Substitute Equation (17) into (12), we have

$$\Gamma \propto \frac{\dot{M}_{\rm acc}}{\dot{M}_{\rm jet}} a^2 \propto a^2, \tag{19}$$

if the mass loss rate in the jets $\dot{M}_{\rm jet}$ is assumed to be proportional to the mass accretion rate $\dot{M}_{\rm acc}$. The correlation between black hole mass and the bulk Lorentz factor of the jet components found in this work implies that the motion velocity of the jet components is probably governed by the black hole spin, if the massive black holes are spinning more rapidly than the less massive counterparts. This is consistent with the magnetically arrested accretion flow model (see Equation 19). The bulk Lorentz factor of the jets is predicted to be independent of the accretion rate in this model, which is also consistent with our statistic results (see Figure 4).

In Figure 8 we find that the magnetic energy flux is far less than bulk kinetic power. As discussed in Section 2, the kinetic luminosity $L_{\rm kin}$ will change with a factor of 3 if an electron-proton jet with $\gamma_{\rm min} = 100$ is assumed, so the kinetic energy flux always dominates over magnetic energy flux in the jets of this blazar sample.

In inhomogeneous jet model, the relativistically moving plasma expands uniformly, which suffers adiabatic losses. The electron energy in the jet at parsec scales requires electron acceleration, otherwise huge energy of electrons is required at the base of jet. The magnetic field in the jet may be the energy reservoir for electrons. We see in figure 8 that a few sources have magnetic field energy larger than the kinetic energy of particles. However, in either case of the matter content, most of the sources have kinetic energy of electrons exceeding the magnetic energy. From equation 7 we see that the ratio between proton energy and electron energy is $m_{\rm p}/(\gamma_{\rm e,min} m_{\rm e})$, which is larger than unity in all cases of minimum electron energy discussed in Section 2. Thus, the only energy source for accelerating electrons should be the kinetic energy of protons and such acceleration process would occur in shock process. The electrons are preheated up to average energy of protons heated in the shocks, and then the energy is converted from protons to electrons in the diffusive shock acceleration process (e.g., Amato & Arons 2006; Amano & Hoshino 2009; Sironi & Spitkovsky 2011). Several authors have investigated these scenarios, both analytically and in particle-in-cell simulations (Amato & Arons 2006; Amano & Hoshino 2009; Sironi & Spitkovsky 2011). From this point of view, the electron-proton content is preferred for this sample of radio loud quasars, or at least the electron-proton dominates dynamically over the electron-position pair content. As discussed that in Section 2, only the normalization is changed if the different plasma composition is considered, which means that most of the statistic results derived in this work is independent of the jet composition.

No correlation is found between the Eddington ratio and the Lorentz factor of the jet, which implies that the jet acceleration may not be related to the properties of the accretion disk. The results imply that the BZ mechanism may dominate over the BP mechanism for jet acceleration at least in radio-loud. Laor (2000) found that the black holes in RL AGNs are systematically heavier than those in radio-quiet counterparts, which may imply that heavy black holes are spinning rapidly, and therefore the jets can be easily accelerated by the field lines threading the horizons of these black holes. This is roughly consistent with the conclusion of this work.

The origin of the chaotic magnetic fields in the jets is still unclear. The jets are accelerated by the magnetic fields near the black hole horizon or those threading the rotational accretion disk. It is therefore reasonable to postulate that the strength of the field in the jets is related to the field driving the jets in some way. No significant correlation is present between the magnetic field strength at $10R_{\rm S}$ and the bulk Lorentz factor of the jet components Γ. The independence of the bulk velocity of the jets on the magnetic field strength implies that the Lorentz factor of the jet components is mainly governed by the black hole spin.

Acknowledgments

We thank the referee for his/her helpful comments. This work is supported by the National Basic Research Program of China (grant 2009CB824800), the NSFC (grants 11173043, 11073039, 11121062 and 10833002), and the CAS/SAFEA International Partnership Program for Creative Research Teams (KJCX2-YW-T23).

REFERENCES

Amato, E., & Arons, J. 2006, ApJ, 653, 325

Amano, T., & Hoshino, M. 2009, ApJ, 690, 244

Barth, A. J., Ho, L. C., & Sargent, W. L. W. 2003, ApJ, 583, 134

Blandford, R. D., Königl, A. 1979, ApJ, 232, 34

Blandford, R. D., & Payne, D. G. 1982, MNRAS, 199, 883

Blandford, R. D., & Znajek, R. L. 1977, MNRAS, 179, 433

Blundell, K. M., Fabian, A. C., Crawford, C. S., Erlund, M. C., & Celotti, A. 2006, ApJ, 644, L13

Cao, X. 2003, ApJ, 599, 147

Cao, X. 2011, ApJ, 737, 94

Cao, X., & Jiang, D. R. 1999, MNRAS, 307, 802

Cao, X., & Jiang, D. R. 2001, MNRAS, 320, 347

Cao, X., & Li, F. 2008, MNRAS, 390, 561

Celotti, A., & Fabian, A. C. 1993, MNRAS, 264, 228

Celotti, A., Padovani, P., & Ghisellini, G. 1997, MNRAS, 286, 415

Fan, Z.-H., & Cao, X. 2004, ApJ, 602, 103

Ghisellini, G., Padovani, P., Celotti, A., & Maraschi, L. 1993, ApJ, 407, 65

Ghosh, P., & Abramowicz, M. A. 1997, MNRAS, 292, 887

Godfrey, L. E. H., Bicknell, G. V., Lovell, J. E. J., et al. 2009, ApJ, 695, 707

Gu, M., Cao, X., & Jiang, D. R. 2009, MNRAS, 396, 984

Guijosa, A., & Daly, R. A. 1996, ApJ, 461, 600

Gültekin, K., Cackett, E. M., Miller, J. M., et al. 2009, ApJ, 706, 404

Hirotani, K. 2005, ApJ, 619, 73

Hughes, S. A., & Blandford, R. D. 2003, ApJ, 585, L101

Jiang, D. R., Cao, X., & Hong, X. 1998, ApJ, 494, 139

Kawakatu, N., Imanishi, M., & Nagao, T. 2007, ApJ, 661, 660

Kellermann, K. I., Lister, M. L., Homan, D. C., et al. 2004, ApJ, 609, 539

Kellermann, K. I., Sramek, R., Schmidt, M., Shaffer, D. B., & Green, R. 1989, AJ, 98, 1195

Kim, M., Ho, L. C., Peng, C. Y., et al. 2008, ApJ, 687, 767

Kino, M., Kawakatu, N., & Takahara, F. 2012, ApJ, 751, 101

Kino, M., & Takahara, F. 2004, MNRAS, 349, 336

Königl, A. 1981, ApJ, 243, 700

Lähteenmäki, A., & Valtaoja, E. 1999, ApJ, 521, 493

Laor, A. 2000, ApJ, 543, L111

Li, S.-L., & Cao, X. 2012, ApJ, 753, 24

Liang, E. W., & Liu, H. T. 2003, MNRAS, 340, 632

Lister, M. L., & Homan, D. C. 2005, AJ, 130, 1389

Liu, Y., Jiang, D. R., & Gu, M. F. 2006, ApJ, 637, 669

Livio, M., Ogilvie, G. I., & Pringle, J. E. 1999, ApJ, 512, 100

Marscher, A. P. 1987, Superluminal Radio Sources, 280

McKinney, J. C., Tchekhovskoy, A., & Blandford, R. D. 2012, MNRAS, 423, 3083

McLure, R. J., & Dunlop, J. S. 2001, MNRAS, 327, 199

Moderski, R., & Sikora, M. 1996, MNRAS, 283, 854

Netzer, H. 1990, Active Galactic Nuclei, 57

Oshlack, A. Y. K. N., Webster, R. L., & Whiting, M. T. 2002, ApJ, 576, 81

Panessa, F., Bassani, L., Cappi, M., et al. 2006, A&A, 455, 173

Park, K., & Blackman, E. G. 2010, MNRAS, 403, 1993

Peterson, B. M., Ferrarese, L., Gilbert, K. M., et al. 2004, ApJ, 613, 682

Pian, E., Falomo, R., & Treves, A. 2005, MNRAS, 361, 919

Rawlings, S., Saunders, R., Eales, S. A., & Mackay, C. D. 1989, MNRAS, 240, 701

Readhead, A. C. S. 1994, ApJ, 426, 51

Reynolds, C. S., Fabian, A. C., Celotti, A., & Rees, M. J. 1996, MNRAS, 283, 873

Shen, Y., Greene, J. E., Strauss, M. A., Richards, G. T., & Schneider, D. P. 2008, ApJ, 680, 169

Shields, G. A., Gebhardt, K., Salviander, S., et al. 2003, ApJ, 583, 124

Sikora, M., & Madejski, G. 2000, ApJ, 534, 109

Sironi, L., & Spitkovsky, A. 2011, ApJ, 726, 75

Soltan, A. 1982, MNRAS, 200, 115

Stawarz, Ł., Cheung, C. C., Harris, D. E., & Ostrowski, M. 2007, ApJ, 662, 213

Tavecchio, F., Maraschi, L., Sambruna, R. M., & Urry, C. M. 2000, ApJ, 544, L23

Tchekhovskoy, A., & McKinney, J. C. 2012, MNRAS, 423, L55

Tchekhovskoy, A., Narayan, R., & McKinney, J. C. 2011, MNRAS, 418, L79

Tremaine, S., Gebhardt, K., Bender, R., et al. 2002, ApJ, 574, 740

Vitrishchak, V. M., Gabuzda, D. C., Algaba, J. C., et al. 2008, MNRAS, 391, 124

Volonteri, M., Sikora, M., & Lasota, J.-P. 2007, ApJ, 667, 704

Wardle, J. F. C., Homan, D. C., Ojha, R., & Roberts, D. H. 1998, Nature, 395, 457

Woo, J.-H., & Urry, C. M. 2002, ApJ, 579, 530

Woo, J.-H., Urry, C. M., van der Marel, R. P., Lira, P., & Maza, J. 2005, ApJ, 631, 762

Wu, Q. 2009, MNRAS, 398, 1905

Wu, X.-B., Liu, F. K., & Zhang, T. Z. 2002, A&A, 389, 742

Zhou, M., & Cao, X.-W. 2009, Research in Astronomy and Astrophysics, 9, 293

This preprint was prepared with the AAS LaTeX macros v5.2.

Table 1. Data for the sample.

Source (1)	Class (2)	z (3)	log Γ (4)	n_1 (cm^{-3}) (5)	B_1 (gauss) (6)	log $M_{\rm BH}$ ($M_\odot$) (7)	Refs. (8)	log $L_{\rm BLR}$ (erg s^{-1}) (9)
0007+106	Qc	0.089	0.279	1.32E+04	0.030	8.29	K07	44.14
0016+731	Qc	1.781	1.248	6.75E+04	0.546	8.93	Z09	44.98
0035+413	Qc	1.353	1.283	5.01E+06	0.724	8.53	Z09	44.64
0106+013	Qc	2.107	1.378	1.15E+05	0.687	8.83	Z09	46.15
0112−017	Qc	1.365	0.230	9.52E+04	0.089	7.85	Z09	45.26
0133+207	Ql	0.425	1.456	2.09E+06	0.230	9.45	L06	45.02
0133+476	Qc	0.859	0.568	4.42E+04	0.254	8.30	Z09	44.47
0153+744	Qc	2.338	1.090	2.23E+06	0.227	9.82	S03	46.14
0202+149	Qc	0.405	0.820	1.63E+04	0.240	9.60	L03	···
0208−512	Qc	1.003	1.505	2.07E+04	0.753	9.21	F04	45.19
0212+735	Qc	2.367	0.924	5.06E+05	0.498	6.96	L06	44.95
0219+428	BL	0.444	1.580	1.89E+04	0.201	8.60	L03	···
0235+164	BL	0.940	1.823	1.37E+05	2.125	10.22	W04	43.86
0316+413	G	0.017	0.114	4.76E+03	0.012	8.51	P06	42.70
0333+321	Qc	1.263	1.439	1.01E+05	0.543	9.25	L06	45.93
0336−019	Qc	0.852	1.294	9.73E+03	0.404	8.98	W02	45.00
0420−014	Qc	0.915	1.193	1.01E+05	0.466	8.41	L06	44.92
0430+052	G	0.033	0.778	3.43E+02	0.019	7.74	P04	42.93
0440−003	Qc	0.844	1.462	2.89E+05	0.526	8.81	F04	44.77
0458−020	Qc	2.286	1.140	4.42E+04	0.376	8.66	F04	45.32
0528+134	Qc	2.060	1.588	3.32E+05	1.187	10.20	L03	···
0605−085	Qc	0.872	1.127	4.77E+05	0.579	8.43	Z09	44.62
0607−157	Qc	0.324	0.591	1.39E+04	0.196	7.32	L06	43.56
0716+714	BL	0.300	1.695	6.91E+04	0.258	8.10	L03	···
0723+679	Ql	0.846	1.185	3.82E+05	0.420	8.67	W02	44.80
0735+178	BL	0.424	1.401	4.70E+04	0.353	8.40	C03	···
0736+017	Qc	0.191	1.090	1.05E+03	0.096	8.47	M01	44.18
0738+313	Qc	0.630	0.431	2.64E+04	0.126	9.40	W02	45.78
0745+241	Qc	0.409	0.934	1.20E+04	0.166	7.92	S08	···

Table 1—Continued

Source (1)	Class (2)	z (3)	log Γ (4)	n_1 (cm^{-3}) (5)	B_1 (gauss) (6)	log $M_{\rm BH}$ ($M_\odot$) (7)	Refs. (8)	log $L_{\rm BLR}$ (erg s^{-1}) (9)
0748+126	Qc	0.889	1.121	2.69E+04	0.394	8.15	L06	44.95
0754+100	BL	0.266	1.107	8.83E+03	0.145	10.14	C03	···
0804+499	Qc	1.432	0.944	6.67E+04	0.279	9.39	L06	45.39
0823+033	BL	0.506	1.164	8.33E+03	0.183	8.83	C03	43.40
0827+243	Qc	0.939	1.507	1.23E+05	0.568	9.80	L03	44.93
0829+046	BL	0.180	1.246	1.97E+03	0.111	8.46	W05	···
0836+710	Qc	2.172	1.467	1.50E+06	0.607	9.36	L06	46.43
0850+581	Qc	1.322	1.575	2.02E+06	0.275	8.49	L06	45.66
0851+202	BL	0.306	1.155	1.87E+04	0.147	8.79	C03	43.60
0859−140	Ql	1.339	1.225	4.13E+04	0.379	8.87	Z09	45.74
0906+015	Qc	1.018	1.086	7.05E+04	0.461	8.55	L06	45.11
0906+430	Qc	0.670	1.041	2.95E+03	0.191	7.90	W02	43.34
0917+449	Qc	2.180	1.117	8.70E+04	0.297	9.31	S08	45.21
0923+392	Qc	0.695	1.637	1.77E+07	0.801	9.28	W02	45.79
0945+408	Qc	1.252	1.356	1.55E+04	0.388	8.60	L06	45.59
0953+254	Qc	0.712	1.350	1.39E+05	0.373	9.00	W02	44.97
0954+658	BL	0.368	1.013	4.17E+03	0.115	8.53	F04	42.63
1012+232	Qc	0.565	0.968	5.70E+03	0.197	8.69	Z09	45.16
1015+359	Qc	1.226	1.182	1.07E+05	0.461	9.11	S08	45.98
1040+123	Qc	1.029	1.072	1.10E+06	0.461	8.76	L06	45.11
1055+018	Qc	0.888	0.740	2.80E+04	0.338	8.45	Z09	44.53
1101+384	BL	0.031	0.519	1.67E+03	0.008	8.22	W05	41.40
1127−145	Qc	1.187	1.843	9.81E+05	1.161	9.18	Z09	45.77
1128+385	Qc	1.733	0.322	7.96E+04	0.169	9.29	S08	46.26
1137+660	Ql	0.646	0.708	6.98E+05	0.110	9.31	L06	45.85
1156+295	Qc	0.729	1.346	1.05E+04	1.107	8.54	L06	44.90
1219+285	BL	0.102	0.845	1.12E+04	0.054	7.40	L03	42.25
1222+216	Ql	0.435	1.438	1.21E+04	0.253	8.44	F04	44.73
1226+023	Qc	0.158	1.436	1.29E+05	0.274	8.95	P04	45.59

Table 1—Continued

Source (1)	Class (2)	z (3)	log Γ (4)	n_1 (cm^{-3}) (5)	B_1 (gauss) (6)	log $M_{\rm BH}$ ($M_\odot$) (7)	Refs. (8)	log $L_{\rm BLR}$ (erg s^{-1}) (9)
1253−055	Qc	0.538	1.017	3.83E+04	0.391	8.28	L06	44.64
1302−102	Qc	0.286	0.799	1.33E+04	0.075	8.58	K08	44.91
1308+326	BL	0.996	1.656	4.41E+04	0.934	9.24	W04	45.12
1334−127	Qc	0.539	0.991	1.06E+04	0.373	7.98	L06	44.18
1345+125	G	0.121	0.806	5.13E+05	0.235	7.80	W09	···
1406−076	Q	1.494	1.786	1.01E+05	0.948	9.40	L03	45.47
1458+718	Qc	0.905	1.117	4.58E+04	0.271	8.77	L06	45.47
1508−055	Ql	1.191	1.639	8.48E+04	0.566	8.97	Z09	45.52
1510−089	Qc	0.360	1.446	4.26E+04	0.345	8.65	W02	44.65
1532+016	Qc	1.420	1.696	5.15E+06	1.074	8.73	Z09	44.84
1546+027	Qc	0.412	0.380	1.85E+04	0.095	8.31	O02	44.68
1606+106	Qc	1.226	1.631	1.57E+05	1.106	9.50	L03	···
1611+343	Qc	1.401	1.919	1.07E+06	1.603	9.60	L06	45.91
1618+177	Ql	0.555	1.013	1.17E+06	0.158	9.65	L06	46.13
1622−297	Q	0.815	1.328	6.06E+04	0.669	9.10	L03	···
1633+382	Qc	1.814	1.196	9.90E+04	0.443	9.67	L06	45.84
1637+826	G	0.023	0.041	4.94E+02	0.007	8.78	G09	···
1641+399	Qc	0.593	1.470	5.91E+05	1.043	9.42	W02	45.47
1642+690	Qc	0.751	1.223	6.14E+03	0.265	7.76	W02	43.86
1652+398	BL	0.034	0.623	1.24E+04	0.019	8.62	W05	41.36
1655+077	Qc	0.621	1.442	2.28E+05	0.698	7.28	L06	43.62
1656+053	Qc	0.879	0.898	1.12E+06	0.297	9.62	W02	46.26
1721+343	Ql	0.205	1.161	7.05E+05	0.101	8.04	W02	44.63
1730−130	Qc	0.902	1.418	1.32E+05	0.756	9.30	L03	44.83
1749+096	BL	0.320	0.949	2.62E+03	0.271	8.34	Z09	···
1749+701	BL	0.770	1.072	2.29E+04	0.208	10.39	C03	···
1803+784	BL	0.684	0.041	1.04E+05	0.079	7.92	L06	44.56
1807+698	BL	0.051	1.021	6.15E+02	0.054	8.51	B03	41.40
1823+568	BL	0.664	0.672	2.95E+04	0.200	9.26	Wu02	43.32

Table 1—Continued

Source (1)	Class (2)	z (3)	log Γ (4)	n_1 (cm^{-3}) (5)	B_1 (gauss) (6)	log $M_{\rm BH}$ ($M_\odot$) (7)	Refs. (8)	log $L_{\rm BLR}$ (erg s^{-1}) (9)
1828+487	Ql	0.692	1.176	1.30E+04	0.237	9.85	L06	45.25
1845+797	Qc	0.057	0.580	1.02E+04	0.018	8.46	P04	42.97
1921−293	Qc	0.352	0.954	3.90E+05	0.146	8.38	Z09	43.67
1928+738	Qc	0.302	1.061	6.88E+03	0.181	8.91	W02	45.18
2131−021	BL	1.285	0.892	7.38E+04	0.365	10.21	C03	43.66
2134+004	Qp	1.932	0.322	3.41E+05	0.195	8.50	Z09	46.29
2145+067	Qc	0.999	0.556	8.31E+04	0.335	8.87	L06	45.78
2200+420	BL	0.069	0.845	6.27E+02	0.049	8.23	W02	42.38
2201+315	Qc	0.298	0.851	8.23E+03	0.095	8.43	W02	45.46
2223-052	Qc	1.404	1.520	4.53E+04	0.606	8.54	Z09	45.62
2230+114	Qc	1.037	1.446	5.51E+04	0.476	8.64	Z09	45.89
2243−123	Qc	0.630	1.100	7.80E+04	0.352	8.32	P05	45.28
2251+158	Qc	0.859	1.511	1.67E+05	0.493	9.17	W02	45.68
2345−167	Qc	0.576	0.204	3.55E+04	0.091	8.47	L06	44.38

Note. — Column (1): IAU name; Column (2): classification of the source (Q=quasars; Qc=core-dominated quasars; Ql=lobe-dominated quasars; Qp=GHz peaked quasars; BL=BL Lac objects; G=radio galaxies). Column (3): redshift. Column (4): the jet Lorentz factor Γ. Column(5): density of electrons n_1. Column(6): magnetic field strength. Column (7): black hole mass. Column (8): references for black hole mass. Column (9): the total luminosity in broad emission lines $L_{\rm BLR}$.

References. — B03: Barth et al. (2003); C03: Cao (2003); F04: Fan & Cao (2004); G09: Gültekin et al. (2009); K07: Kawakatu et al. (2007); K08: Kim et al. (2008); L03: Liang & Liu (2003); L06: Liu et al. (2006); M01: McLure & Dunlop (2001); O02: Oshlack et al. (2002); P04: Peterson et al. (2004); P05: Pian et al. (2005);

P06: Panessa et al. (2006); S03: Shields et al. (2003); S08:Shen et al. (2008); W02: Woo & Urry (2002); W05: Woo et al. (2005); W09: Wu (2009); Wu02: Wu et al. (2002); Z09: Zhou & Cao (2009);

Table 2. Spearman Partial Rank Correlation Analysis of the Sample

Sample (1)	N (2)	Correlation:A,B (3)	Variable:C (4)	$r_{\rm AB}$ (5)	significance level(%) (6)	$r_{\rm AB,C}$ (7)	significance (8)
All	101	$M_{\rm BH}$,Γ	z	0.357	99.98	0.240	2.41
		Γ,z	$M_{\rm BH}$	0.385	99.99	···	···
		$M_{\rm BH}$,z	Γ	0.400	99.99	···	···
Quasars	77	$M_{\rm BH}$,Γ	z	0.376	99.92	0.305	2.70
		Γ,z	$M_{\rm BH}$	0.311	99.41	···	···
		$M_{\rm BH}$,z	Γ	0.327	99.63	···	···
with $L_{\rm BLR}$	87	$L_{\rm bol}/L_{\rm Edd}$,Γ	z	0.099	63.94	···	···
sources within $0.8 < z < 1.2$	23	$M_{\rm BH}$,Γ	z	0.590	99.64	0.580	2.89
		Γ,z	$M_{\rm BH}$	0.243	73.54	···	···
		$M_{\rm BH}$,z	Γ	0.132	45.01	···	···

Note. — Here $r_{\rm AB}$ is the rank correlation coefficient of the two variables, and $r_{\rm AB,C}$ is the partial rank correlation coefficient. Column (6) is the significance level of the rank correlation. Column (8) is the significance of the partial rank correlation equivalent to the deviation from a unit variance normal distribution if there is no correlation present.

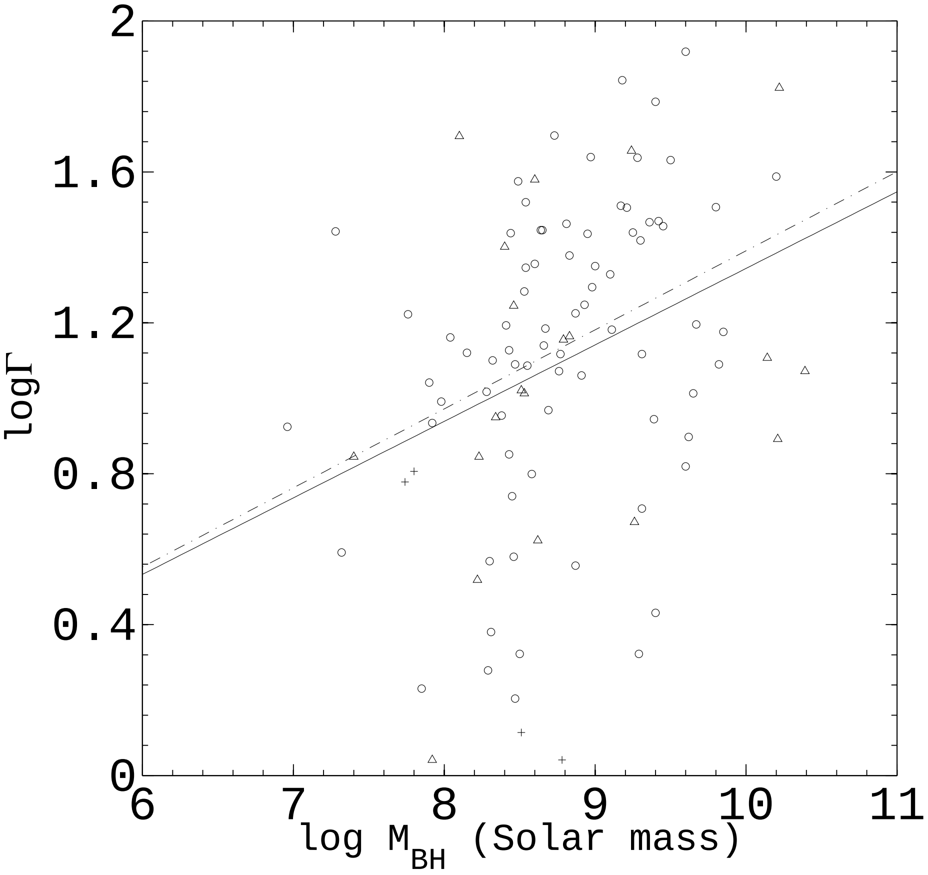

Fig. 1.— The relation between black hole mass and the bulk Lorentz factor of the jet components. The circles represent quasars, and the triangle represents BL Lac objects, while the crosses represent radio galaxies. The solid line is the fitted line for the whole sample using the least square method while the dot-dashed line is fitted for quasars only.

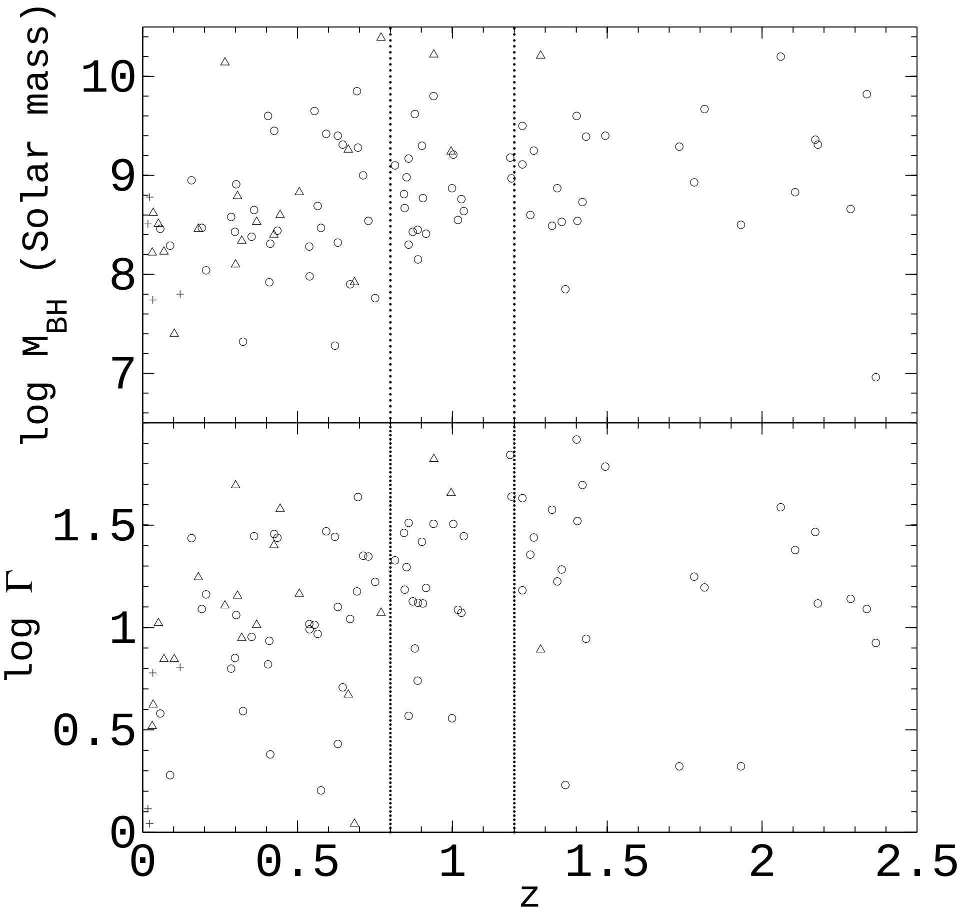

Fig. 2.— The relation between black hole mass and redshift z (the upper panel). The lower panel is the relation between the bulk Lorentz factor of the jet components and redshift z. The two vertical dotted lines correspond to $z = 0.8$ and 1.2, respectively.

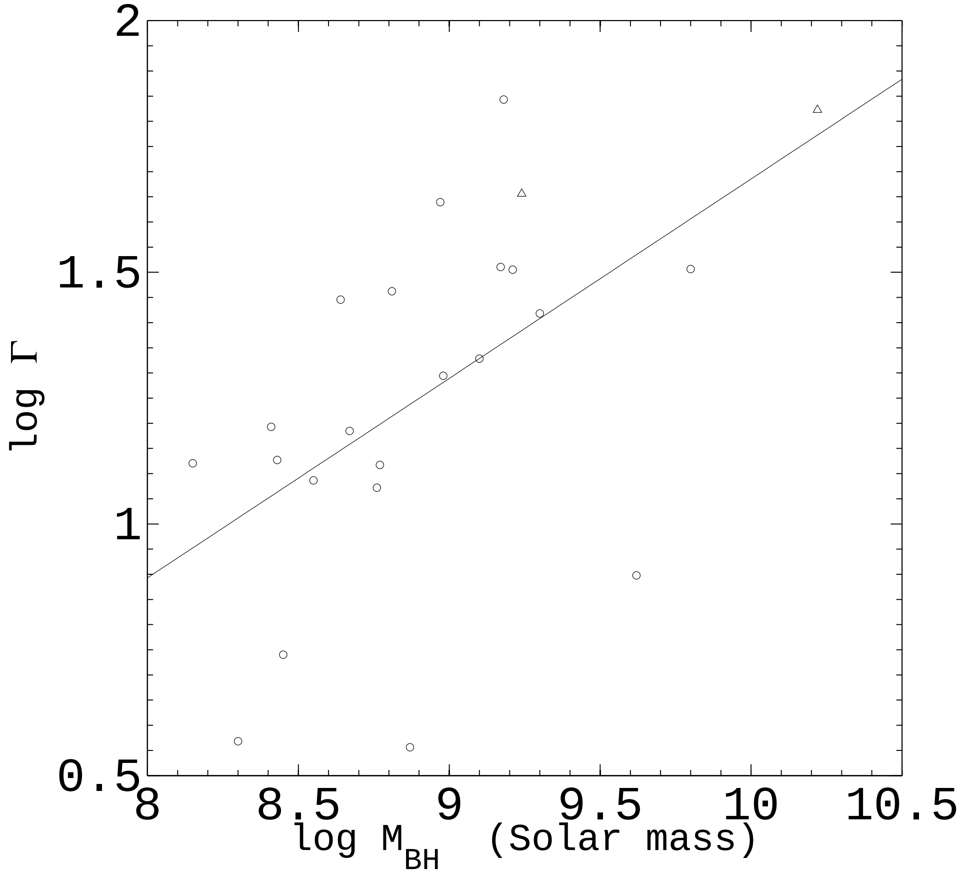

Fig. 3.— The relation between black hole mass and the bulk Lorentz factor of the jet components for the sub-sample of the sources with redshift $0.8 < z < 1.2$. The symbols are the same as Figure 1.

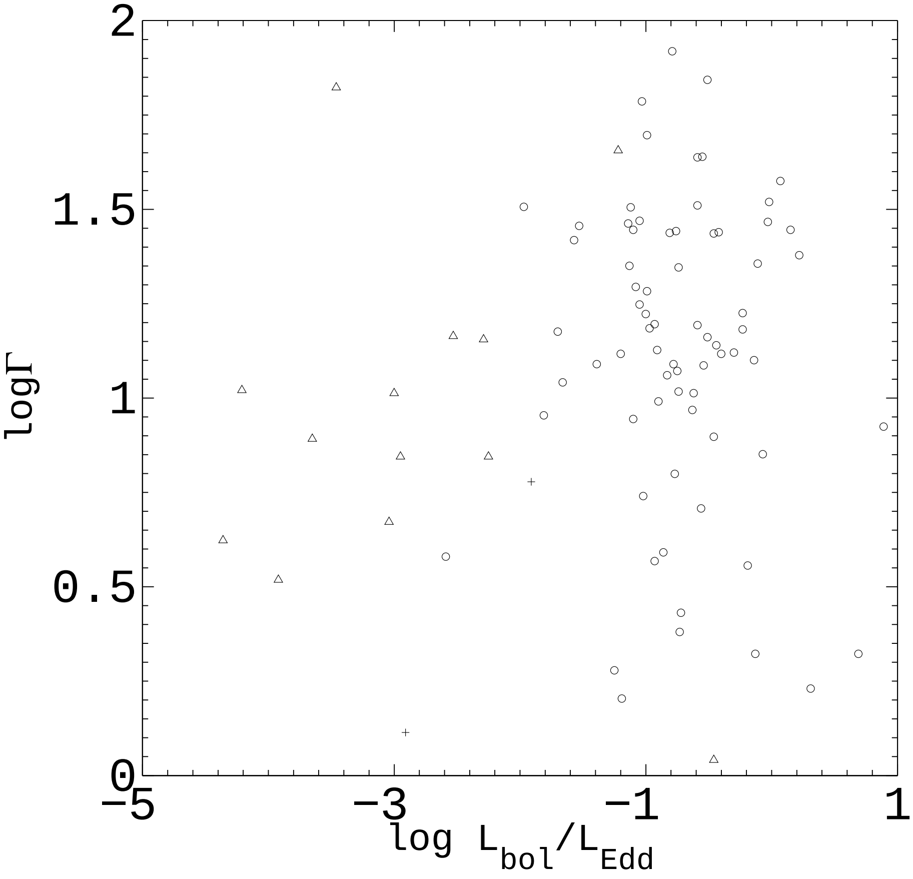

Fig. 4.— The relation between the Eddington ratio and the bulk Lorentz factor of jet. The symbols are the same as Figure 1.

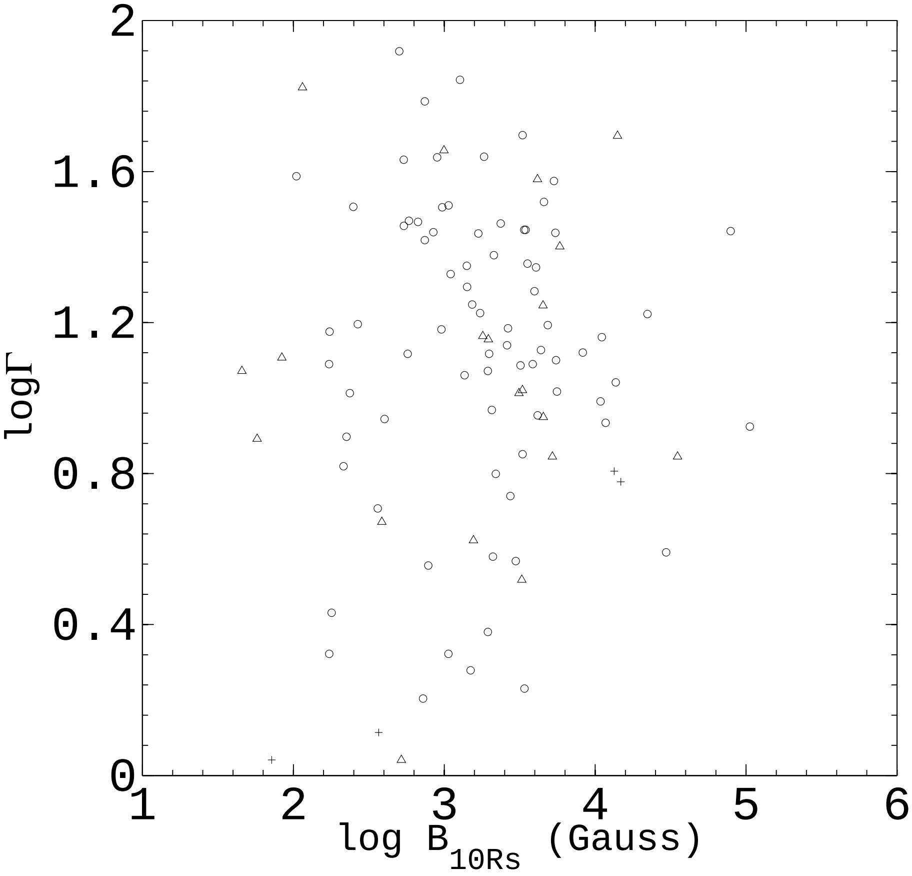

Fig. 5.— The relation between magnetic field strength at $10R_{\rm S}$ and the bulk Lorentz factor of jet. The symbols are the same as Figure 1.

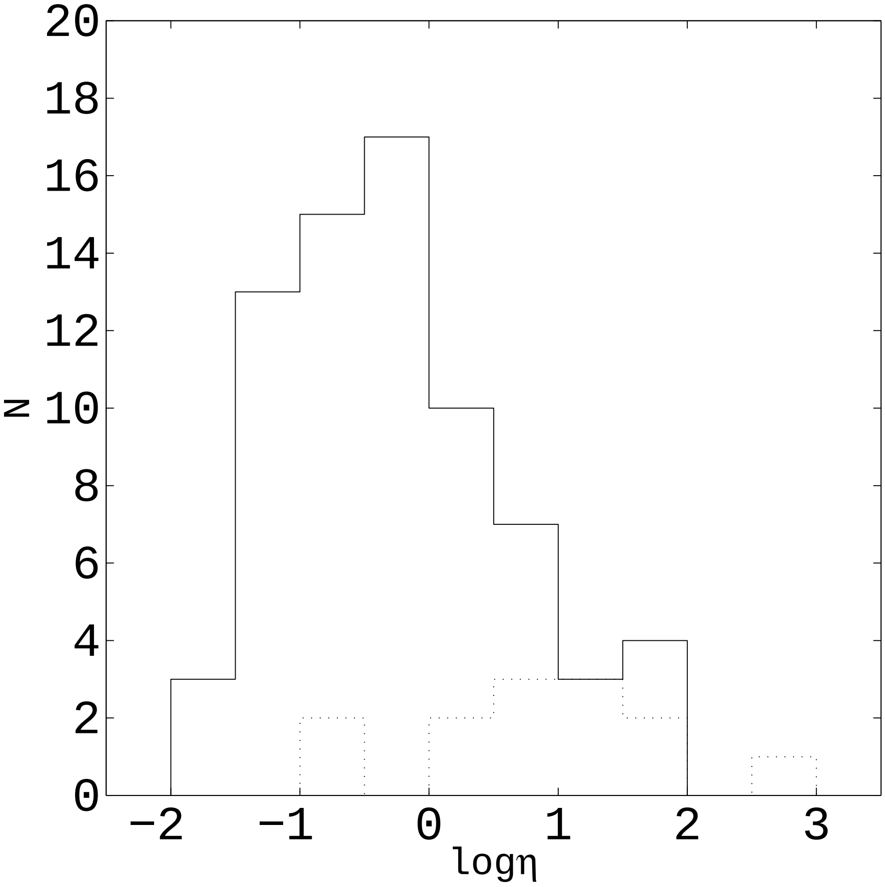

Fig. 6.— The distribution of jet efficiency $\eta_{\rm jet}$ (solid line: quasars, and dotted line: BL Lac objects).

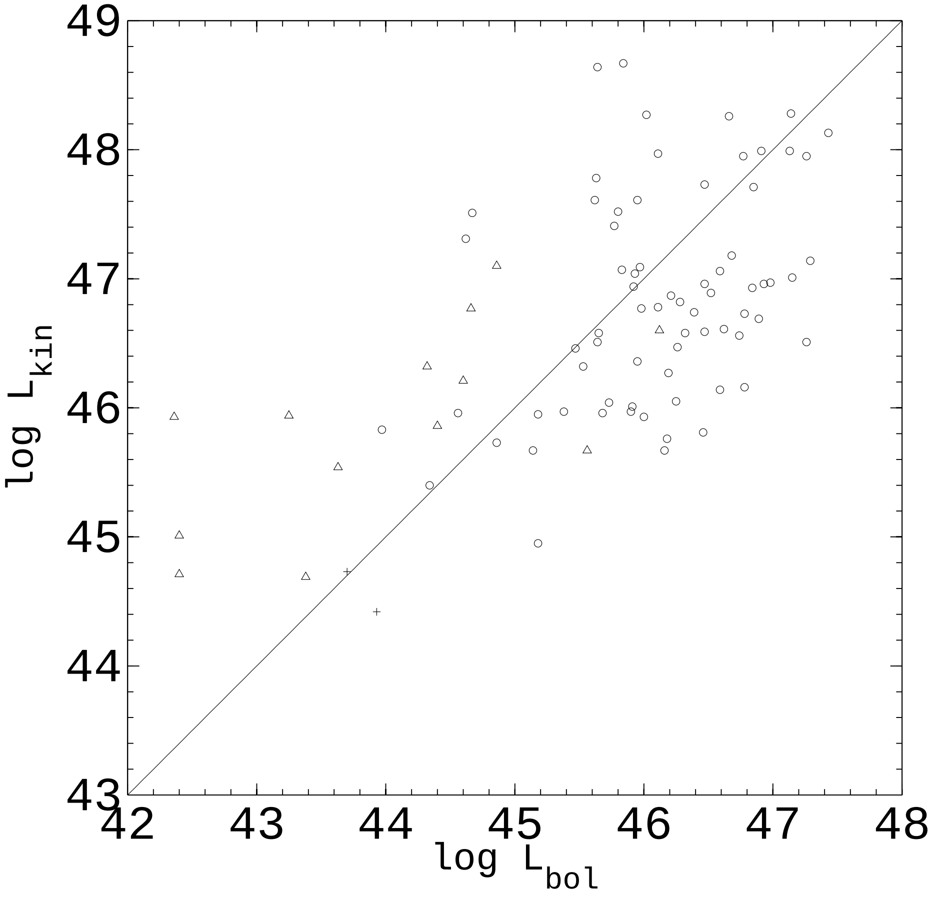

Fig. 7.— The relation between bolometric luminosity and kinetic power of jets. The line correspond to jet efficiency of η=1. The symbols are the same as Figure 1.

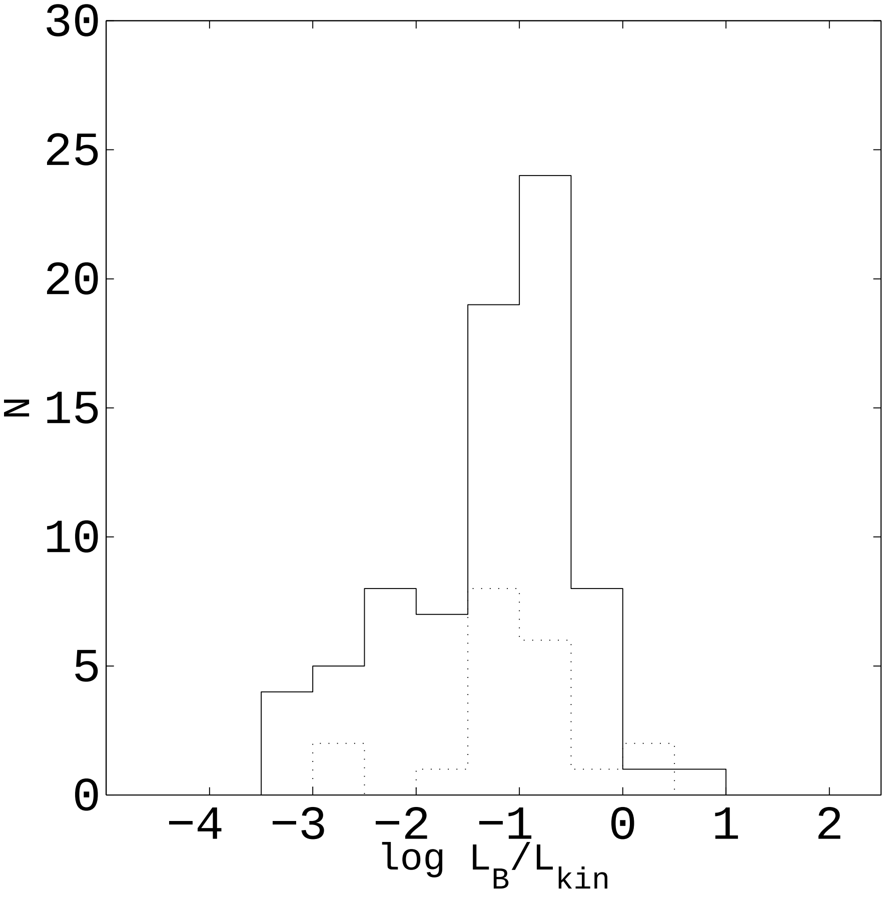

Fig. 8.— The distribution of radio between magnetic energy flux and bulk kinetic power (solid line: quasars, and dotted line: BL Lac objects).